

Published in final edited form as:

*J Orthop Res.* 2013 November ; 31(11): 1765–1771. doi:10.1002/jor.22421.

## Contrast Enhanced CT Attenuation Correlates with the GAG Content of Bovine Meniscus

Bejamin A. Lakin<sup>1,2</sup>, Daniel J. Grasso<sup>1</sup>, Rachel C. Stewart<sup>1,2</sup>, Jonathan D. Freedman<sup>1,2</sup>, Brian D. Snyder<sup>2,3</sup>, and Mark W. Grinstaff<sup>1</sup>

<sup>1</sup>Department of Biomedical Engineering and Chemistry, Boston University, Boston, Massachusetts

<sup>2</sup>Center for Advanced Orthopaedic Studies, Beth Israel Deaconess Medical Center, Harvard Medical School, Boston, Massachusetts

<sup>3</sup>Children's Hospital, Boston, Massachusetts

### Abstract

We determined whether contrast-enhanced computed tomography (CECT) attenuation obtained using a  $\mu$ CT scanner correlated with the glycosaminoglycan (GAG) content and distribution in ex vivo bovine menisci. Bovine samples were immersed in different concentrations of the contrast agents CA4+ and Ioxaglate, and the  $\mu$ CT images were compared to Safranin-O staining. CA4+ and Ioxaglate diffusion-in kinetics and the correlation between their CECT attenuations and GAG content were investigated. CA4+ and Ioxaglate both reached steady state in the meniscal regions within 95 h, with tau values of  $20.6 \pm 3.98$  and  $25.9 \pm 3.71$  h (mean  $\pm$  SD), respectively. Both agents diffused preferentially through the proximal and secondarily through the distal surface. The CA4+ CECT attenuation was strongly and positively correlated with the GAG content of the meniscus regions ( $R^2 = 0.89$ ,  $p < 0.001$ ) at low concentrations (12 mgI/ml), while the Ioxaglate CECT attenuation was moderately and negatively correlated with the GAG content ( $R^2 = 0.51$ ,  $p = 0.03$ ) at 60 mgI/ml. CECT can image ex vivo menisci, and the CA4+, compared to Ioxaglate, enhanced attenuation strongly correlates with the GAG content and distribution in bovine meniscus.

### Keywords

computed tomography; GAG; bovine; meniscus; osteoarthritis

The menisci are crescent-shaped fibrocartilaginous tissues located in most vertebrates' knee joints. The menisci stabilize the knee joint, absorb shocks, protect the articular cartilage from excessive stress, and are principally composed of water (70–75%), collagens (20–25%), and proteoglycans (1–2%).<sup>1,2,3</sup> Meniscal collagen—principally Type I<sup>2</sup>—forms bundles that resist tensile and shear forces arising during locomotion,<sup>1,4</sup> while the internal proteoglycans and their associated glycosaminoglycan (GAG) side chains bond to water. All of these components contribute to its compressive strength.<sup>1,2,4</sup> Similar to articular cartilage degeneration, meniscus degeneration is associated with osteoarthritis (OA), and the menisci are often damaged during knee OA, first resulting in GAG depletion and, finally, in irreversible collagen damage.<sup>5</sup> Thus, a number of groups are investigating new repair strategies (e.g., tissue engineered constructs).<sup>4,6,7</sup>

A non-destructive imaging technique for examining meniscal biochemical composition and structure is important from a basic science, pre-clinical, and clinical perspective. Imaging modalities used to evaluate the meniscus include MRI and computed tomography (CT).<sup>8,9</sup> MRI is the clinical standard for examining meniscus morphology, including detection of lesions and evaluation of treatment post-operatively using native<sup>8,10,11</sup> and contrast-enhanced MRI.<sup>12-14</sup> However, no studies have reported the correlations between meniscal GAG content and MRI signal.

Unlike MRI, CT is more widely available, is relatively inexpensive, has higher resolution, does not require specialized pulse sequences, can image patients with metal implants, and is more comfortable for patients due to fast acquisition times and minimal enclosure. Although CT imaging uses ionizing radiation, newer scanners can maintain high resolution with lower doses<sup>15</sup> for imaging the knee. Clinically, CT arthrography is used to diagnose meniscal tears.<sup>8,9</sup> There are no in vivo or ex vivo reports of correlations between CT attenuation and meniscal GAG content. However, contrast-enhanced CT (CECT) can measure changes in the GAG content of cartilage utilizing contrast agents<sup>16</sup> that partition in proportion to the GAG content of the cartilage matrix. For example, changes in the X-ray attenuation of cartilage in the presence of Ioxaglate or Iothalamate can be used to quantify the GAG content of normal and degraded articular cartilage.<sup>17-20</sup> Recently, studies reported a new, cationic contrast agent (CA4+) for CECT cartilage imaging<sup>21-24</sup> and the soft callus of fractures.<sup>25</sup> Ioxaglate and CA4+ have the same number of iodine atoms per molecule<sup>6</sup> and similar molecular weights and sizes, while Ioxaglate has one formal negative charge, and CA4+ has four formal positive charges (see Supplemental Information). CECT using CA4+ is a more sensitive technique for monitoring changes in cartilage GAG content and can be accomplished at low contrast agent concentrations.

Since GAGs are an important component of the meniscus, this study determined if CECT can image bovine menisci. We hypothesized that a lower concentration of CA4+ than Ioxaglate can be used to depict GAG distribution, and that the CECT attenuation following immersion in CA4+ or Ioxaglate correlates with GAG content. Herein, we describe the diffusion-in characteristics of Ioxaglate and CA4+ into ex vivo bovine menisci, the distribution of contrast agents within the tissue, and the correlations between CECT attenuation and GAG content.

## METHODS

### Material/Specimen Preparation and Study Design

Eight medial and five lateral menisci were excised from skeletally mature bovine knees and sectioned into three regions: anterior, central, and posterior<sup>3,4,26</sup> (Fig. 1A). Each region served as one sample, and all samples and contrast agents were then prepared as described in the Supplemental Information, for three studies: (1) a diffusion-in study to determine the immersion time required for both Ioxaglate (Hexabrix320, Mallinckrodt, St. Louis, MO) and the cationic contrast agent CA4+ to reach steady state within the different anatomic regions of the meniscus; (2) a concentration optimization study with additional regions to determine the optimal concentration of CA4+ and Ioxaglate to depict the GAG distribution in bovine menisci; and (3) a CECT versus GAG correlation study for Ioxaglate and CA4+. The samples used in each study are summarized in Table 1.

### Contrast Enhanced Computed Tomography (CECT) Imaging

For the diffusion-in study, two posterior, one central, and one anterior samples (Table 1) were immersed in 30 ml solutions of CA4+ at 12 mgI/ml, while one posterior, one central, and two anterior samples were immersed in 30 ml solutions of Ioxaglate at 60 mgI/ml. Both

sets of samples were imaged using CECT at various time points up to 95 h. The time required for the contrast agent to reach equilibrium within the different regions was determined as the time at which the change in CECT attenuation was  $<0.25\%/h$ , corresponding to a 1,000-fold decrease from the original rate of change. The diffusion-in CECT attenuation versus time data were then fit to an exponential:  $CECT\_attenuation = a \times \exp(-b \times time) + c$  (MATLAB 2011a, MATLAB, Natick, MA), and a  $\tau$ -value was computed that represented the time at which 63.2% of the equilibrium attenuation was reached.<sup>20</sup> Once the steady-state immersion time was determined for both agents, five more samples (Table 1) were immersed to equilibrium in 30 ml of five concentrations (12, 24, 48, 60, and 80 mgI/ml) of Ioxaglate. Simultaneously, three regions neighboring the samples used for Ioxaglate (Table 1) were immersed in 30 ml of three concentrations of CA4+ (6, 12, and 24 mgI/ml) to enable direct qualitative comparisons between the distributions of both contrast agents within the meniscus at various concentrations.

From the results of the first and second studies, we determined that immersing samples to equilibrium in CA4+ at 12 mgI/ml generated CECT color maps that qualitatively best reflected the GAG distribution in the bovine meniscus as determined by Safranin-O stained histological slices (described below), while samples immersed in Ioxaglate at 60 mgI/ml reflected the GAG distribution. Thus, for the final study, six more samples (Table 1) were immersed to equilibrium in 30 ml of CA4+ at 12 mgI/ml to provide additional samples for examining the correlation between CA4+ CECT attenuation and GAG content. To compare the Ioxaglate CECT attenuation versus GAG content, nine regions (Table 1) were immersed to equilibrium in 30 ml of Ioxaglate at 60 mgI/ml and CECT scanned. For all studies, each sample was imaged on a  $\mu$ CT system at an isotropic voxel resolution of  $36 \mu m^3$  ( $\mu$ CT40, Scanco Medical AG, Brüttsellen, Switzerland), as described in the Supplemental Information. Following CECT, the imaged zone of each meniscus was excised from the surrounding tissue (Fig. 1B) and immersed in saline for 24 h to wash out the contrast agent.

### Histological and Biochemical Assessment of GAG

Four meniscus regions neighboring those used in Study 2 were analyzed using Safranin-O staining to determine the distribution of GAGs in the regions, as described in the Supplemental Information. The excised meniscus imaging zones from Studies 1 and 3 were cut into three subregions (inner, middle, and outer)<sup>4</sup> (Fig. 1C), and their GAG contents were determined using the DMMB assay as described in the Supplemental Information.

### Statistical Analysis

Since multiple samples were extracted from each knee, a multivariate linear regression was first applied to examine if knee origin and GAG content were strong predictors of CECT attenuation. Since origin was not a strong predictor, univariate linear regression (SPSS 17.0, Chicago, IL) was applied to evaluate whether the CECT attenuation correlated with the entire GAG content of the samples. One-way ANOVA was used to test for differences in GAG content by region and by subregion. Significance level was set as 2-tailed  $p$ -value  $< 0.05$ .

## RESULTS

### Diffusion of Ioxaglate and CA4+ into Bovine Menisci Regions

The CECT attenuation rapidly increased during the first 10 h of immersion for both Ioxaglate and CA4+, with the rate of increase eventually decreasing to  $<0.25\%/h$  after 95 h (Fig. 2A). The  $\tau$ -values were  $20.6 \pm 3.98$  h (mean  $\pm$  SD) for CA4+ and  $25.9 \pm 3.71$  h for Ioxaglate. Since CECT attenuation is a measure of contrast agent concentration, representative color maps from the same imaging slice of a medial, anterior region over the

course of the diffusion-in study (Fig. 2B) indicated that the diffusion of CA4+ (and Ioxaglate; not shown) occurred preferentially through the proximal and secondarily through the distal surface, with minimal diffusion through the medial surface.

### Comparison of Ioxaglate and CA4+ Distributions in the Meniscus

After immersion of a sample in Ioxaglate at 12 mgI/ml for 95 h, the contrast agent was uniformly distributed throughout the tissue cross-section, as determined by the CECT attenuation (Fig. 3A). Repeating the procedure at 24 mgI/ml, the contrast accumulated in the inner and outer subregions of the tissue (Fig. 3B). Increasing the Ioxaglate concentrations to 48 and 60 (Fig. 3C and D, respectively) and 80 mgI/ml (not shown) afforded even greater concentrations in the inner and outer subregions. The CECT images obtained with Ioxaglate at higher concentrations only partially reflected the inverse of the GAG distribution observed with neighboring histological sections (one of the four neighboring histological sections is shown in Fig. 3H). Following immersion of a sample in CA4+ at 6 mgI/ml for 95 h, a greater CECT attenuation was observed in the inner subregion and the proximal and distal portions of the middle subregion, albeit the CECT attenuation in these subregions was not substantial compared to the outer subregion (Fig. 3E). The CECT attenuation was the greatest in the inner and middle subregions for a sample immersed in CA4+ at 12 mgI/ml (Fig. 3F). The same distribution pattern was observed for a sample immersed in CA4+ at 24 mgI/ml, although the CECT attenuation was much greater in the inner subregion and the proximal and distal portions of the middle subregion (Fig. 3G). Histological slices from neighboring regions to these regions showed that the GAG content of bovine menisci was highly concentrated in the inner subregion, followed by the middle subregion (an example is shown in Fig. 3H). Also, the DMMB assay indicated that the GAG concentration in the inner and middle subregions was greater than in the outer subregion for all meniscus regions (Fig. 3I).

### CECT Attenuation versus GAG Content

Following immersion in Ioxaglate at 60 mgI/ml, the CECT attenuation was moderately and negatively correlated with the GAG content of the meniscus regions ( $R^2 = 0.51$ ,  $p = 0.03$ ) (Fig. 4A). After exposure to CA4+ at 12 mgI/ml, the CECT attenuation was strongly and positively correlated with the GAG content of the meniscus regions, accounting for 89% of the variation in GAG content ( $p < 0.001$ ), (Fig. 4B).

## DISCUSSION

We investigated whether CECT imaging can quantify the GAG content and distribution in ex vivo bovine meniscus samples. An imaging method for evaluating meniscus biochemical composition, analogous to those for articular cartilage, may enable early diagnosis of knee OA and provide opportunities to monitor disease progression. Figure 2A shows the diffusion-in kinetics of the cationic contrast agent CA4+ and the anionic agent Ioxaglate into four bovine meniscus regions. The CECT attenuation reached 971 HU for CA4+ and 2,248 HU for Ioxaglate following 95 h of diffusion, reflecting the difference in initial concentration used for each agent (CA4+: 12 mgI/ml and Ioxaglate: 60 mgI/ml). Tau values of  $20.6 \pm 3.98$  h for CA4+ and  $25.9 \pm 3.71$  h for Ioxaglate represent the time at which 63.2% of the final attenuation was reached. Although there are no prior reports of contrast agent diffusion kinetics into ex vivo meniscus, CT contrast agents reach equilibrium within 24 h in articular cartilage specimens.<sup>19-21</sup> Tau values for such agents diffusing into cartilage range from 1.08 to 4.49 h.<sup>20,21</sup> Our slower diffusion-in for meniscus is likely a result of the larger size and lower permeability of the meniscal samples compared to articular cartilage samples. This is supported by a report that the meniscus is about one-sixth as permeable as cartilage<sup>2</sup>

due to the heavily  $\alpha$ -linked collagen fibers around its surface,<sup>27</sup> and that the volume of the meniscus samples is about 30× larger than 7-mm diameter cartilage plugs.

The contrast agents diffused preferentially through the proximal and secondarily through the distal surface, with minimal diffusion through the medial surface (Fig. 2B). This is likely due to the anisotropic arrangement of collagen fibers throughout the meniscus, with the tightest bundles located in the outer subregions.<sup>1,27</sup> Following intra-articular injection, the contrast agent would be exposed to the proximal and distal surfaces of the meniscus, thus permitting the agent to diffuse into the tissue. While a 95-h exposure period is not feasible clinically, human menisci are about one-third the size of bovine menisci, which should reduce the diffusion time; however, this must be confirmed. Asking a patient to walk (as is done clinically for dGEMRIC<sup>13,14</sup>) may accelerate the contrast agent uptake via mechanical convection.

Next, we evaluated the effect of contrast agent charge and concentration on equilibrium partitioning within the meniscus. Color maps from CECT images of various meniscus regions immersed in five concentrations of Ioxaglate (Fig. 3A–D) did not adequately reflect the natural GAG distribution of bovine meniscus as determined by histology and the DMMB assay (Fig. 3H and I). At 12 mgI/ml (Fig. 3A), the contrast agent distribution was essentially homogeneous throughout the meniscus [mean CECT attenuation by subregion: Inner (I): 633 HU, Middle (M): 601 HU, Outer (O): 649 HU]. Higher concentrations of agent showed up to 43% increased signal in both the outer and inner subregions compared to the middle subregion (Fig. 3B–D), despite the higher GAG concentration in the inner subregion (Fig. 3H and I). Ioxaglate diffuses poorly into the middle and deep zones in articular cartilage, where the majority of the GAGs are concentrated,<sup>18,19,21,22</sup> with only partial penetration into the deeper cartilage at concentrations as high as 80 mgI/ml.<sup>17</sup> The penetration of Ioxaglate into the inner subregion of the meniscus (e.g., mean CECT attenuations for Ioxaglate at 60 mgI/ml: I: 2,236 HU, M: 1,928 HU, O: 2,479 HU) is likely due to the lower concentration of GAG in this subregion (2–3%, Fig. 3I) compared to the greater concentration of GAG in the deeper cartilage tissue (4–6%).<sup>17</sup> After immersion in the cationic contrast agent CA4+ at 6 mgI/ml (Fig. 3E), the CA4+ was essentially homogeneously distributed throughout the meniscus (mean CECT attenuations: I: 725 HU, M: 616 HU, O: 406 HU). However, immersions in concentrations of 12 and 24 mgI/ml (similar to those used with articular cartilage<sup>18,21,24</sup>) clearly reflected the GAG distribution in the meniscus (Fig. 3H), with higher CECT attenuation in the middle and inner subregions than the outer subregion (12 mgI/ml: I: 1,692 HU, M: 1,123 HU, O: 661 HU and 24 mgI/ml: I: 2,318 HU, M: 1,648 HU, O: 1,054 HU) (Fig. 3F and G).

The imaging signal differences we observed between the subregions with CA4+ differ from other reports. With dGEMRIC, Krishnan et al.<sup>14</sup> showed no difference in inner, middle, and outer subregions for T1(Gd) following intravenous Gd-DPTA<sup>2-</sup> injection. Li et al.<sup>13</sup> also found no difference in T1(Gd) among subregions. These results may be due to the limited vascularization of meniscus and the much lower GAG content compared to cartilage. The GAG content of the subregions (Fig. 3I) agree with the findings of Ionescu et al. for bovine meniscus<sup>4</sup> and the pattern for sheep and rabbit.<sup>26</sup>

The moderate, negative correlation between the Ioxaglate enhanced CECT attenuation and the GAG content of the meniscus regions ( $R^2 = 0.51$ ,  $p = 0.03$ , Fig. 4A), and the strong, positive correlation between the CA4+ enhanced CT attenuation and the GAG content of the meniscus regions ( $R^2 = 0.89$ ,  $p < 0.001$ , Fig. 4) agree with the relationships reported for these contrast agents in articular cartilage.<sup>17,18,20,21,24</sup> In this study with CA4+ at 12 mgI/ml, CECT attenuations ranged from 850 to 1,300 HU with GAG from 0.8% to 2.5%, while CECT attenuations ranged from 2,100 to 2,600 HU with GAG from 0.7% to 1.7% for



Ioxaglate at 60 mgI/ml. The Ioxaglate CECT attenuation range is similar to that obtained with Ioxaglate at 80 mgI/ml in cartilage (1,600–3,000 HU for 0–5% GAG range),<sup>17</sup> and the CA4+ attenuation range is similar to that with CA4+ at 12 mgI/ml for cartilage (1,000–2,000 HU for 1.4–2.9% GAG range).<sup>24</sup> The slopes of –32,045 for Ioxaglate and 24,543 for CA4+ relating CECT attenuation to GAG content of bovine meniscus are also comparable to those reported for cartilage (Ioxaglate: slope = –30,132 at 80 mgI/ml,<sup>17</sup> CA4+ slope = 19,936 at 12 mgI/mL<sup>24</sup>), indicating a similar sensitivity to meniscal GAG content. However, the CECT attenuation using CA4+ at a lower concentration accounted for more of the variability in GAG content than did the CECT attenuation following Ioxaglate exposure (89% vs. 51%). Thus, CECT can quantify the GAG content in both articular cartilage and meniscus.

In this study, extracted regions from intact menisci were used to provide a wide range of GAG contents and to enable more reproducible imaging. These regions are not representative of the native geometry of the meniscus. However, the cross-sectional geometry was maintained, and the cut ends were sealed to ensure diffusion only through native surfaces. These menisci were frozen and thawed twice, which could increase their permeability and the diffusion rate of the contrast agents into the samples. Even though we demonstrated proof of principle, a 95-h exposure time is not clinically feasible. In vivo, the diffusion of the contrast agents may be accelerated by mechanical convection (e.g., a patient walking) and body temperature, which may decrease the time required to reach equilibrium in tissue.

In OA, both cartilage and meniscus progressively degrade, resulting in a loss of GAGs, increased hydration, and fibrillation of the extracellular matrix. These alterations affect tissue function; hence, a diagnostic capable of monitoring biochemical changes may enable detection of OA before severe damage occurs. Since CECT attenuation correlates with GAG content of cartilage and now, for the first time, with GAG content in meniscus, CECT permits quantitative GAG analysis of two critical soft tissues involved in OA. Importantly, since subchondral bone attenuates X-rays and is also affected by OA,<sup>28</sup> CECT enables simultaneous evaluation of both soft tissues and the bone for comprehensive monitoring and diagnosis of the disease.

## Supplementary Material

Refer to Web version on PubMed Central for supplementary material.

## Acknowledgments

Grant sponsor: Coulter Foundation; Grant sponsor: Harvard Catalyst Program; Grant sponsor: NIH; Grant number: R01GM098361; Grant sponsor: BU Undergraduate Research Opportunities Program; Grant sponsor: Henry Luce Foundation.

The authors thank Dr. Entezari for help with the study design. This work was supported in part by the Coulter Foundation, the Harvard Catalyst Program, the NIH (R01GM098361), the BU Undergraduate Research Opportunities Program (D.J.G.), and the Henry Luce Foundation (R.C.S.). M.W.G. and B.D.S. have a COI via a submitted patent application (M.W.G.) and grant funding from the NIH (M.W.G. and B.D.S.).

## References

1. Mow, VC.; Huiskes, R. Basic orthopaedic biomechanics & mechano-biology. Philadelphia, PA: Lippincott Williams & Wilkins; 2005.
2. Fithian DC, Kelly MA, Mow VC. Material properties and structure-function relationships in the menisci. Clin Orthop. 1990; 252:19–31. [PubMed: 2406069]
3. Adams ME, Muir H. The glycosaminoglycans of canine menisci. Biochem J. 1981; 197:385–389. [PubMed: 6798964]

4. Ionescu LC, Lee GC, Garcia GH, et al. Maturation state-dependent alterations in meniscus integration: implications for scaffold design and tissue engineering. *Tissue Eng Part A*. 2011; 17:193–204. [PubMed: 20712419]
5. Englund M, Guermazi A, Lohmander SL. The role of the meniscus in knee osteoarthritis: a cause or consequence? *Radiol Clin North Am*. 2009; 47:703–712. [PubMed: 19631077]
6. Baker BM, Gee AO, Sheth NP, et al. Meniscus tissue engineering on the nanoscale: from basic principles to clinical application. *J Knee Surg*. 2009; 22:45–59. [PubMed: 19216353]
7. Makris EA, Hadidi P, Athanasiou KA. The knee meniscus: structure-function, pathophysiology, current repair techniques, and prospects for regeneration. *Biomaterials*. 2011; 32:7411–7431. [PubMed: 21764438]
8. Huysse WC, Verstraete KL, Verdonk PC, et al. Meniscus imaging. *Semin Musculoskelet Radiol*. 2008; 12:318–333. [PubMed: 19016395]
9. Toms AP, White LM, Marshall TJ, et al. Imaging the post-operative meniscus. *Eur J Radiol*. 2005; 54:189–198. [PubMed: 15837398]
10. van Heuzen EP, Golding RP, van Zanten TE, et al. Magnetic resonance imaging of meniscal lesions of the knee. *Clin Radiol*. 1988; 39:658–660. [PubMed: 3243058]
11. Gatehouse PD, Thomas RW, Robson MD, et al. Magnetic resonance imaging of the knee with ultrashort TE pulse sequences. *Magn Reson Imaging*. 2004; 22:1061–1067. [PubMed: 15527992]
12. McCauley TR. MR imaging evaluation of the postoperative knee. *Radiology*. 2005; 234:53–61. [PubMed: 15564389]
13. Li W, Edelman RR, Prasad PV. Delayed contrast enhanced MRI of meniscus with ionic and non-ionic agents. *J Magn Reson Imaging*. 2011; 33:731–735. [PubMed: 21563259]
14. Krishnan N, Shetty SK, Williams A, et al. Delayed gadolinium-enhanced magnetic resonance imaging of the meniscus: an index of meniscal tissue degeneration? *Arthritis Rheum*. 2007; 56:1507–1511. [PubMed: 17469113]
15. Gervaise A, Louis M, Batch T. Dose reduction at CT of the lumbar spine using a 320-detector row scanner: initial results. *J Radiologie*. 2010; 91:779–785.
16. Lusic H, Grinstaff MW. X-ray computed tomography contrast agents. *Chem Rev*. 2013; 113:1641–1666. [PubMed: 23210836]
17. Bansal PN, Joshi NS, Entezari V, et al. Contrast enhanced computed tomography can predict the glycosaminoglycan content of and biomechanical properties of articular cartilage. *Osteoarthritis Cartilage*. 2010; 18:184–189. [PubMed: 19815108]
18. Bansal PN, Stewart RC, Entezari V, et al. Contrast agent electrostatic attraction rather than repulsion to glycosaminoglycans affords a greater contrast uptake ratio and improved quantitative CT imaging in cartilage. *Osteoarthritis Cartilage*. 2011; 19:970–976. [PubMed: 21549206]
19. Kokkonen HT, Jurvelin JS, Tiitu V, et al. Detection of mechanical injury of articular cartilage using contrast enhanced computed tomography. *Osteoarthritis Cartilage*. 2011; 19:295–301. [PubMed: 21215317]
20. Palmer AW, Guldberg RE, Levenston ME. Analysis of cartilage matrix fixed charge density and three-dimensional morphology via contrast-enhanced microcomputed tomography. *Proc Natl Acad Sci*. 2006; 103:19255–19260. [PubMed: 17158799]
21. Bansal PN, Joshi NS, Entezari V, et al. Cationic contrast agents improve quantification of glycosaminoglycan (GAG) content by contrast enhanced CT imaging of cartilage. *J Orthop Res*. 2011; 29:704–709. [PubMed: 21437949]
22. Joshi NS, Bansal PN, Stewart RC, et al. Effect of contrast agent charge on visualization of articular cartilage using computed tomography: exploiting electrostatic interactions for improved sensitivity. *J Am Chem Soc*. 2009; 131:13234–13235. [PubMed: 19754183]
23. Stewart RC, Bansal PN, Entezari V, et al. Contrast-enhanced computed tomography using a high affinity cationic contrast agent for imaging ex vivo bovine, intact ex vivo rabbit, and in vivo rabbit cartilage. *Radiology*. 2013; 266:130–140. [PubMed: 23169794]
24. Lakin BA, Grasso DJ, Shah SS, et al. Cationic agent contrast-enhanced computed tomography imaging of cartilage correlates with the compressive modulus and coefficient of friction. *Osteoarthritis Cartilage*. 2013; 21:60–68. [PubMed: 23041438]

25. Hayward LN, De Bakker CM-J, Gerstenfeld LC, et al. Assessment of contrast-enhanced computed tomography for imaging of cartilage during fracture healing. *J Orthop Res.* 2013; 31:567–573. [PubMed: 23165442]
26. Chevrier A, Nelea M, Hurtig MB, et al. Meniscus structure in human, sheep, and rabbit for animal models of meniscus repair. *J Orthop Res.* 2009; 27:1197–1203. [PubMed: 19242978]
27. Petersen W, Tillmann B. Collagenous fibril texture of the human knee joint menisci. *Anat Embryol.* 1998; 197:317–324. [PubMed: 9565324]
28. Brandt KD, Radin EL, Dieppe PA, et al. Yet more evidence that osteoarthritis is not a cartilage disease. *Ann Rheum Dis.* 2006; 65:1261–1264. [PubMed: 16973787]



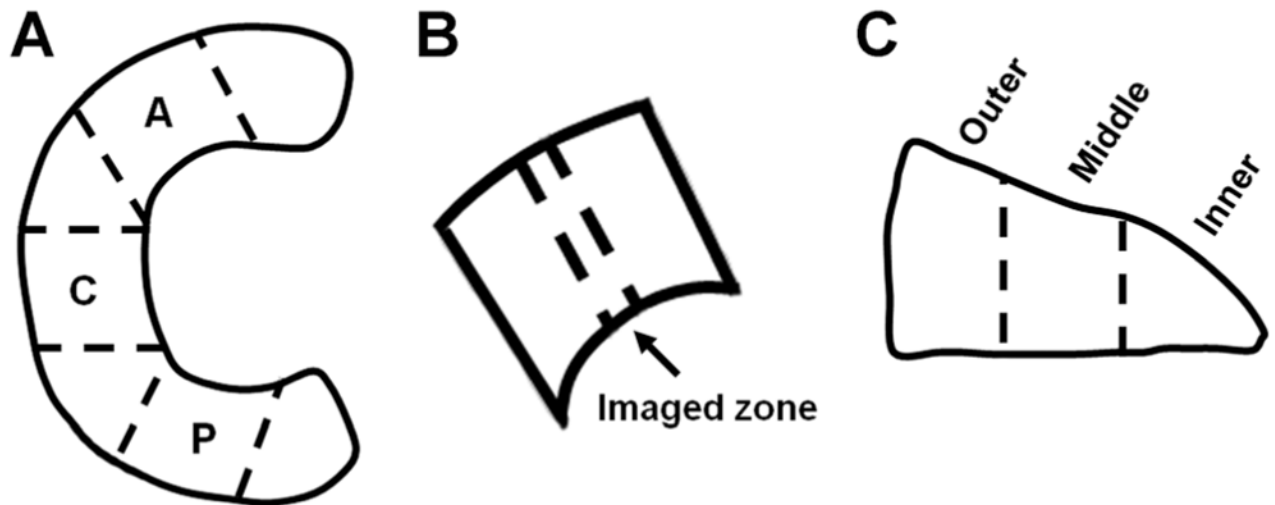


**Figure 1.**

Preparation of the bovine menisci for CECT imaging and biochemical analysis. (A) Schematic displaying how anterior (A), central (C), and posterior (P) regions were harvested from bovine menisci for all three studies. (B) Location of CECT imaged zone in all regions that was also excised for DMMB assay to determine GAG content. (C) Excised CECT imaged zones from samples in the diffusion-in and fixed-immersion time studies were further divided into inner, middle, and outer cross-sectional subregions for determining GAG content in each subregion.

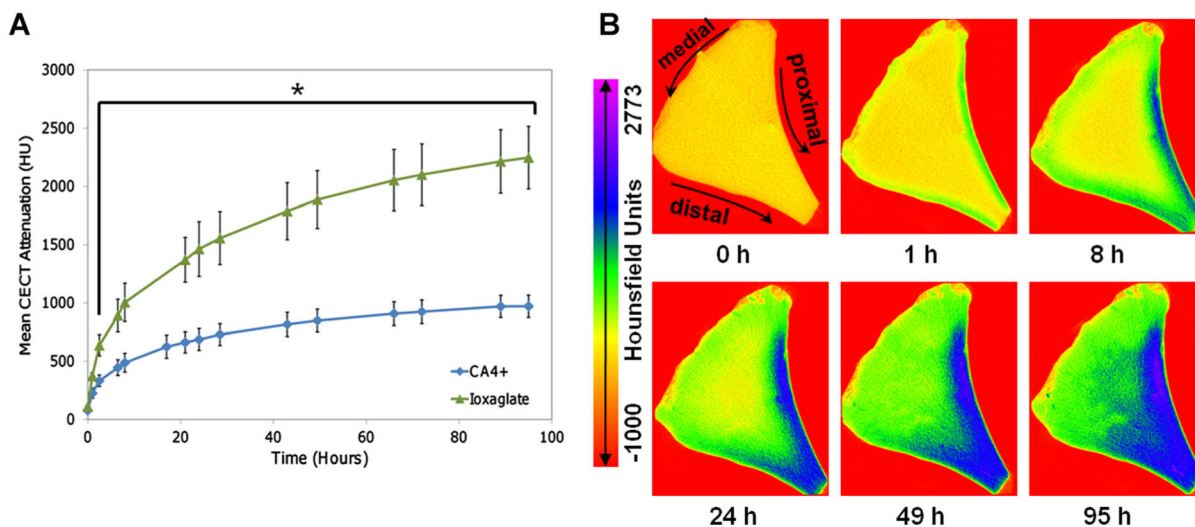


**Figure 2.**

(A) Diffusion-in results for CA4+ and Ioxaglate contrast agents in anterior, central, and posterior regions of bovine meniscus. The curves are for visualization purposes only. The rate of change in CECT attenuation decreased to  $<0.25\%/h$  after 95 h compared to  $>200\%/h$  initially, as the process reached equilibrium. \*The mean CECT attenuation was significantly greater for the Ioxaglate samples than for those immersed in CA4+ for all time points after 1 h ( $p < 0.01$ ). (B) CECT color maps of a cross-sectional slice from an anterior region immersed in CA4+ showing progressing contrast enhancement over 95 h of diffusion.

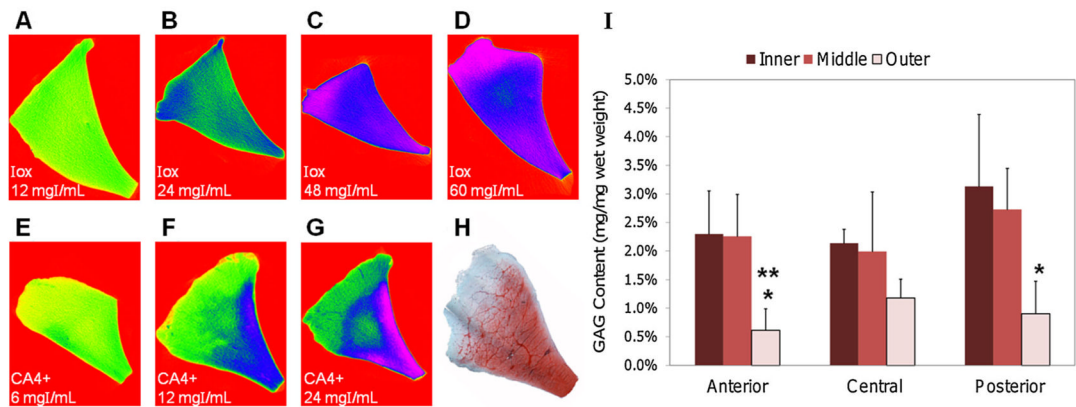


**Figure 3.**

CECT color maps of cross-sectional slices from bovine menisci following 95 h immersions in Ioxaglate (Iox) at (A) 12 mg/ml, (B) 24 mg/ml, (C) 48 mg/ml, (D) 60 mg/ml and in CA4+ at (E) 6 mg/ml, (F) 12 mg/ml, and (G) 24 mg/ml. (H) Representative histological cross-sectional slice from a bovine meniscus stained with Safranin-O to indicate GAG distribution. (I) GAG contents in the inner, middle, and outer subregions of anterior, central, and posterior menisci samples ( $n = 3/\text{region}$ ). \*GAG content lower than posterior inner subregion ( $p < 0.05$ ). \*\*GAG content lower than posterior middle subregion ( $p < 0.05$ ).

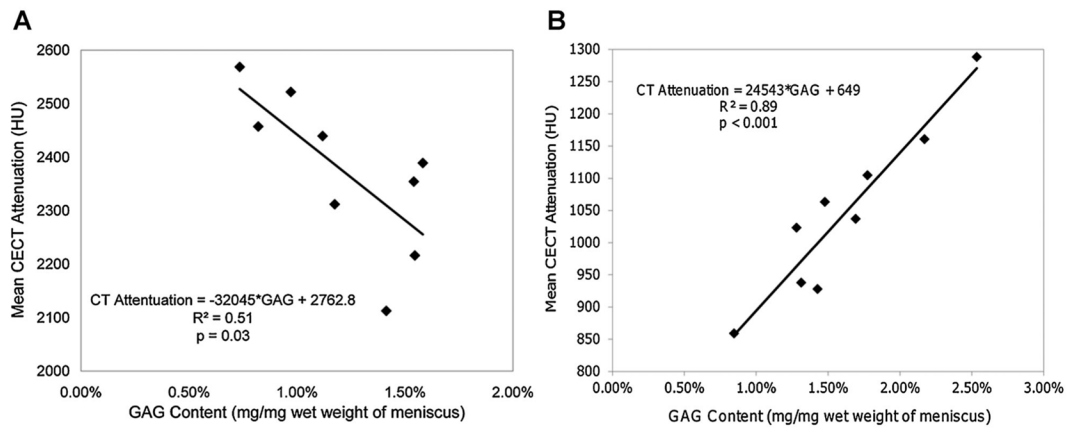


**Figure 4.** Correlations between CECT attenuation (HU) and GAG content (mg/mg) of menisci samples after immersion for 95 h in (A) Ioxaglate ( $n = 9$ ) and (B) the CA4+ contrast agent ( $n = 9$ ).

**Table 1**

Origin of meniscus samples (regions) for each study

<b>Knee Number</b>	<b>1</b>	<b>2</b>	<b>3</b>	<b>4</b>	<b>5</b>	<b>6</b>	<b>7</b>	<b>8</b>	<b>9</b>
<b>Side</b>	M	L	M	M	L	M	L	L	M
<b>Region</b>	A C P	A C P A C P	A C P A C P	A C P A C P	A C P A C P	A C P A C P	A C P A C P	A C P A C P	A C P A C P
<b>Study</b>									
Loxaglate diffusion-In ( <i>n</i> = 4)	X	X				X			X
CA4+ diffusion-In ( <i>n</i> = 4)			X	X	X				
Loxaglate concentration opt. ( <i>n</i> = 5)	B	K	C	J	K		H	A	
CA4+ concentration opt. ( <i>n</i> = 3)	K	E			G	K	H	F	
Loxaglate CECT attenuation vs. GAG ( <i>n</i> = 9)								X	X
CA4+ CECT attenuation vs. GAG ( <i>n</i> = 9)			X	X	X	X	X	X	X

X denotes samples used for given study; A denotes sample shown in Figure 3A; B denotes Figure 3B; C denotes Figure 3C; D denotes Figure 3D; E denotes Figure 3E; F denotes Figure 3F; G denotes Figure 3G; H denotes Figure 3H; J denotes sample immersed in Iox at 80 mg/ml (not shown in Fig. 3); and K denotes sample used for histological analysis and comparison (not shown in Fig. 3).